Adaptive Digital Predistortion of Wireless Power Amplifiers/Transmitters Using Dynamic Real-Valued Focused Time-Delay Line Neural Networks

Meenakshi Rawat, Karun Rawat, *Student Member, IEEE*, and Fadhel M. Ghannouchi, *Fellow, IEEE*

***Abstract*—Neural networks (NNs) are becoming an increasingly attractive solution for power amplifier (PA) behavioral modeling, due to their excellent approximation capability. Recently, different topologies have been proposed for linearizing PAs using neural based digital predistortion, but most of the previously reported results have been simulation based and addressed the issue of linearizing static or mildly nonlinear PA models. For the first time, a realistic and experimentally validated approach towards adaptive predistortion technique, which takes advantage of the superior dynamic modeling capability of a real-valued focused time-delay neural network (RVFTDNN) for the linearization of third-generation PAs, is proposed in this paper. A comparative study of RVFTDNN and a real-valued recurrent NN has been carried out to establish RVFTDNN as an effective, robust, and easy-to-implement baseband model, which is suitable for inverse modeling of RF PAs and wireless transmitters, to be used as an effective digital predistorter. Efforts have also been made on the selection of the most efficient training algorithm during the reverse modeling of PA, based on the selected NN. The proposed model has been validated for linearizing a mildly nonlinear class AB amplifier and a strongly nonlinear Doherty PA with wideband code-division multiple access (WCDMA) signals for single- and multiple-carrier applications. The effects of memory consideration on linearization are clearly shown in the measurement results. An adjacent channel leakage ratio correction of up to 20 dB is reported due to linearization where approximately 5-dB correction is observed due to memory effect nullification for wideband multicarrier WCDMA signals.**

***Index Terms*—Linearization, memory effect, neural network (NN), power amplifier (PA), third-generation (3G) wideband code-division multiple access (WCDMA) signals.**

I. Introduction

LINEARIZATION of nonlinear power amplifiers (PAs) is an important issue with the growing use of advanced modulation and access techniques that utilize spectrally efficient modulation waveforms, such as orthogonal frequency-division multiplexing (OFDM), code-division multiple access (CDMA2000) and wideband code-division multiple access (WCDMA), in communication systems. A PA that works with these wideband signals causes out-of-band emission, also known as spectral regrowth, due to the nonlinear behavior of the PA. Furthermore, PAs are typically operated as close as possible to saturation to achieve maximum power efficiency and output power, which also means functioning in the most nonlinear region, implying significant distortion and spectral regrowth.

As solutions to this efficiency-linearity dilemma, several techniques have been proposed in the literature for the linearization of RF PAs. Linearization techniques, such as feedforward [1]–[3], feedback [4], [5], analog predistortion [6], [7] and their optimized variations are based on analog correction: hence, the implementation of these techniques as a whole transmitter in the base station is cumbersome, due to complex circuitry, stability issues, and insufficient linearization. The digital predistortion (DPD) technique is now a widely accepted and proven linearization approach for base station transmitters and PAs, which is further enabled by recent advances in digital signal processors and digital-to-analog converters (DACs). Furthermore, DPD provides accuracy in synthesizing the predistortion function and in reconfiguration capability due to a software platform that makes it suitable for multistandard environments [8].

The DPD technique relies on the introduction of an exact inverse nonlinear characteristic element (predistorter) before the PA, which compensates for nonlinearity; therefore, the prime concern is a good inverse model. To address this issue, various techniques, are such as lookup table (LUT) [9], [10], Volterra series [11], Weiner Hammerstein [12], and polynomial models [13], [14] have been proposed in the literature and can be considered conventional techniques.

Recently, the novel technique of neural networks (NNs) has attracted researchers in the field of PA modeling due to its successful implementation in pattern recognition, signal processing, system identification, and control [15]–[19]. The NN approach has also been investigated as one of the modeling and predistortion techniques for PAs and transmitters because of its adaptive nature and the claim of a universal approximation capability [20]–[25]. Different neural topologies and computation algorithms have been proposed; and, most of these have been individual efforts that have not been compared in order to establish an optimal model, in terms of robustness, convergence speed, and accuracy. Moreover, the efforts made to propose DPD techniques based on NN modeling lacked experimental validation with real PAs and have not considered memory effects while implementing the models.

Manuscript received July 27, 2009; revised October 18, 2009. First published November 24, 2009; current version published January 13, 2010. This work was supported by the Alberta Informatics Circle of Research Excellence (iCORE), the Natural Sciences and Engineering Research Council of Canada (NSERC), the Canada Research Chair (CRC) Program, and TRLabs.

The authors are with the iRadio Laboratory, Department of Electrical and Computer Engineering, Schulich School of Engineering, University of Calgary, Calgary, AB, Canada T2N 1N4 (e-mail:mrawat@ucalgary.ca; fadhel.ghannouchi@ucalgary.ca).

Color versions of one or more of the figures in this paper are available online at http://ieeexplore.ieee.org.

Digital Object Identifier 10.1109/TMTT.2009.2036334

This paper presents a comparison of different NN topologies and training algorithms that lead to the identification of a model that could establish a suitable and optimal (in terms of fewer parameters and epochs) dynamic reverse model for RF PAs. The real-valued focused time-delay neural network (RVFTDNN) was found to be the most suitable, accurate, and robust model for DPD-based linearization of mildly, as well as strongly, nonlinear PAs. The DPD model based on the proposed dynamic NN is validated for linearizing a class AB amplifier and a Doherty amplifier.

The proposed DPD model based on NN also considers the incorporation of memory effects, which is experimentally validated in terms of adjacent channel leakage ratio (ACLR) reduction and compared to the previously proposed NN-based static models that have not considered memory effects.

Section II describes the previously proposed NN topologies and their limitations, leading to Section III, which discusses the selection procedure for a suitable training algorithm and the robustness of the selected RVFTDNN predistorter from a modeling and adaptation point of view. Section IV describes the predistortion scheme and experimental setup, and experimental results are reported in Section V. The robustness of the proposed model was also tested with various signals to report the backward compatibility of the model.

II. NNs for PA Modeling

When an input signal is uniformly sampled, each sample instant is related to a time sample; and, in NNs, synaptic weights of each neuron are convolved with a sequence of input samples. In this way, the time-dependent structure of the input signal is embedded in the spatial structure of the network for long-term memory.

PA modeling calls for a model that can extract amplitude and phase information from modulated complex waveforms. The most basic structure [20] proposed is a single-input single-output feedforward NN utilizing complex input/output. This topology introduces complex weight and activation outputs, which leads to cumbersome calculations. To address this issue, other topologies utilizing real-valued double-input double-output have been proposed.

Fig. 1(a) presents an NN [21], [22] topology utilizing two uncoupled NNs that attempts to capture amplitude modulation (AM/AM) and phase modulation (AM/PM) responses separately. The main drawback of this topology is the asynchronous convergence of the two NNs, where both NNs do not converge to an optimal model at same time, leading to over- or under-training of one NN. A more effective approach, called the real-valued feedforward neural network (RVFFNN), is shown in Fig. 1(b), which takes advantage of the easy availability of the in-phase (I) component and quadrature (Q) phase component of the modulated waveform in the baseband, thereby saving pre- and post-processing activities and can be used as a common feedforward NN with two inputs and two outputs. Although this topology has been found effective for forward modeling of very nonlinear PAs, it falls short of expectations when the PA shows strong memory effects. For wideband signals, in particular, the role of memory effects cannot be neglected [26].

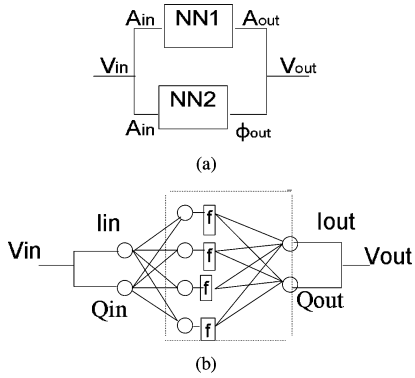

Fig. 1. Conventional real-valued NN topologies for PA modeling. (a) Two NN two-input topology. (b) Two NN one-input topology.

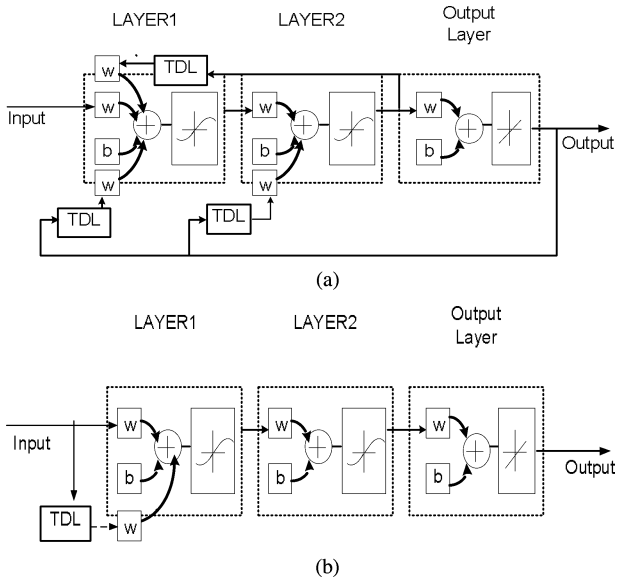

Fig. 2. (a) RNN signal processing scheme. (b) FTDNN signal processing scheme.

To take care of memory effects, two dynamic neural structures have been proposed in the NN literature. In the first, recurrent neural networks (RNNs) utilize feedforward and feedback signal processing. Reference [24] reported PA modeling using a fully connected RNN, which is shown in Fig. 2(a); however, it again uses single-input single-output complex waveforms, and hence, suffers from the drawbacks previously mentioned.

The second technique is a focused time-delay neural network (FTDNN), which relies on the fact that, due to memory effects in the system, the output of the amplifier depends on present, as well as previous, input values. Thus, this technique avoids a feedback time-delay line and extracts information from present and past inputs [25].

The RVFTDNN is a combination of the two-input topology of the RVFFNN shown in Fig. 1(b) and the FTDNN technique given in Fig. 2(b), which was found effective in modeling PAs with strong memory effects.

Therefore, due to their dynamic modeling capability, the real-valued recurrent neural network (RVRNN) and the RVFTDNN are considered here among all the other NN topologies as potential candidates for PA dynamic modeling. In Section III, a comparative study of RVRNN and RVFTDNN topologies is carried

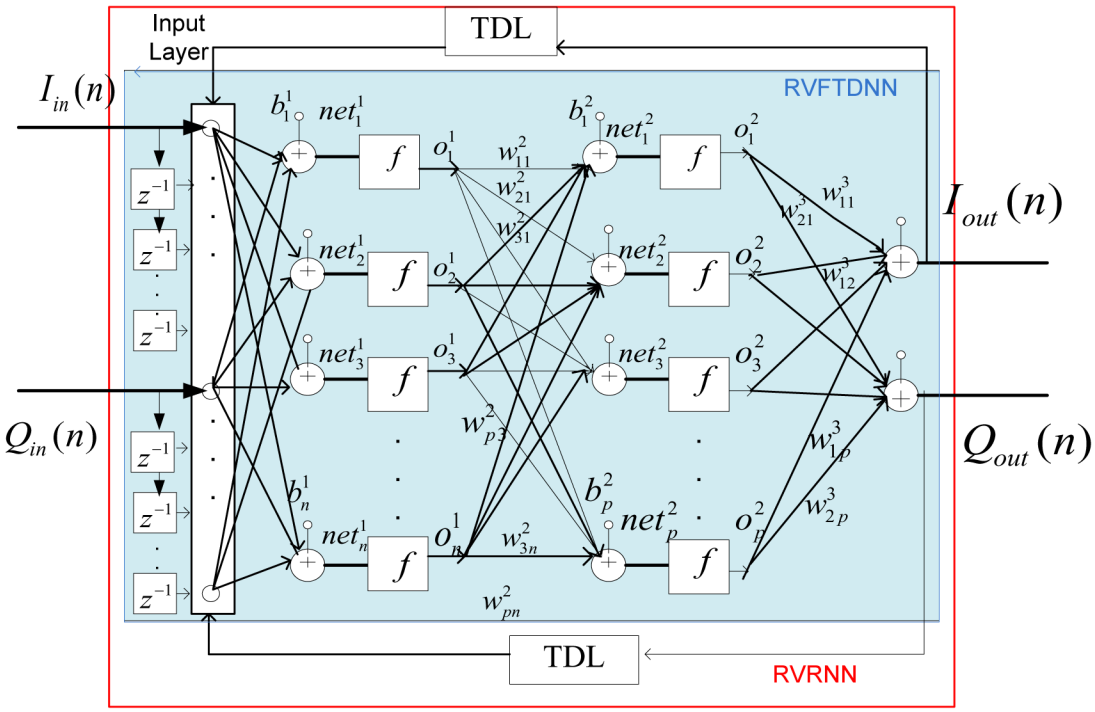

Fig. 3. RVRNN schematic. Shaded portion is attributed to RVFTDNN.

out to establish one of them as the optimal NN model for DPD applications.

III. Selection of Real-Valued NN Dynamic Model

A. Training and Parameter-Extraction Procedure

RVRNN: The significant difference between the RVRNN and RNN proposed in [24] is that the RVRNN is structured to take advantage of the easy availability of I and Q components of the complex waveform in the baseband signals. Furthermore, the training process becomes significantly faster with the use of real weights instead of the complex weights of the RNN. Fig. 3 shows a block diagram of RVRNN signal processing.

At any moment of the training sequence, the NN is presented with input vectors of the order $2(m+t+1)$-by-1, including past inputs and NN outputs

$$\begin{aligned} X_{\text{in}} = [&I_{\text{in}}(n), I_{\text{in}}(n-1)\dots I_{\text{in}}(n-m), \quad Q_{\text{in}}(n), \\ &Q_{\text{in}}(n-1)\dots Q_{\text{in}}(n-m), \\ &I_{\text{out}}(n)\dots I_{\text{out}}(n-t), \\ &Q_{\text{out}}(n), \quad Q_{\text{out}}(n-1)\dots Q_{\text{out}}(n-t)] \end{aligned} \tag{1}$$

where m is the memory depth of the input vector and t is the memory delay length of the feedback signal

$$I_{\text{out}}(n) = f_1(X_{\text{in}}(n)) \tag{2}$$

$$Q_{\text{out}}(n) = f_2(X_{\text{in}}(n)) \tag{3}$$

where f_1 and f_2 are functions modeled by RVRNN at any instant (n).

RVFTDNN: The RVFTDNN signal processing scheme is shown as the shaded portion in Fig. 3. The NN is presented with input vectors of the order $2(m+1)$-by-1, including real values of present and past inputs

$$\begin{aligned} X_{\text{in}} = [&I_{\text{in}}(n), I_{\text{in}}(n-1)\dots I_{\text{in}}(n-m), \\ &Q_{\text{in}}(n), Q_{\text{in}}(n-1)\dots Q_{\text{in}}(n-m)] \end{aligned} \tag{4}$$

The delayed response is achieved by using $\sum_1^m z^{-n}$ as the delay operator, where z^{-1} is the unit delay operator that yields its delayed version $x(n-1)$ when operating on $x(n)$. The tapped delay lines store values from the previous time step, which can be used in the current time step.

The training procedure is similar for both models. When no initial knowledge is assumed, synaptic weights are chosen such that induced local fields of neurons lie at the transition between the linear and saturated parts of the sigmoidal activation. A very high value can drive the network into the saturation part of the activation function making the learning process slow while very small values may lead it to work on a flat region stopping the training for that neuron [16]. To satisfy these requirements, weights are initialized randomly within the interval of $[-0.8, 0.8]$ to avoid extremes values of -1 or 1 of the activation function. Gradually weights converge to their optimal values as the training proceeds. The hidden layers are fully connected, as shown in Fig. 3.

The net at any layer is given by

$$\text{net}_j^l(n) = \sum_{i=1}^{q} w_{ji}^l x_{\text{in},i}^{l-1}(n) + b_j^l \tag{5}$$

where j denotes a neuron in hidden layer l, and w_{ji}^l denotes the synaptic weight connecting the ith input to the jth neuron of layer l.

The output of any layer is given as

$$o_j^l = f(\text{net}_j^l(n)). \tag{6}$$

The output of any layer works as an input for the next layer. The output layer has a purelin activation function, which sums up the outputs of hidden neurons and linearly maps them at the output. The activation function f chosen for two hidden layers is the tansig function, which maps nonlinearity between -1 and 1 and is mathematically equivalent to hyperbolic tangent given as

$$\tanh(x) = \frac{\exp(x) - \exp(-x)}{\exp(x) + \exp(-x)}. \tag{7}$$

Training is carried out in batch mode, supervised with a back-propagation algorithm. Detailed descriptions of back-propagation can be found in [16] and [27]. During one epoch or iteration, two passes are made. During the forward pass, the cost function is calculated by

$$E = \frac{1}{2N}\sum_{n=1}^{N}[(I_{\text{out}}(n) - \hat{I}_{\text{out}}(n))^2 + (Q_{\text{out}}(n) - \hat{Q}_{\text{out}}(n))^2] \tag{8}$$

where $I_{\text{out}}(n)$ and $Q_{\text{out}}(n)$ are the desired outputs, and $\hat{I}_{\text{out}}(n)$ and $\hat{Q}_{\text{out}}(n)$ are the outputs from the NN. Based on the error signal in (5), backward computation is done to adjust the synaptic weights of the network in layer l according to

$$w(n+1) = w(n) + \Delta w(n). \tag{9}$$

In (9), $w(n)$ denotes the weights at a previous time instant, $n, w(n+1)$ is the updated weight, and $\Delta w(n)$ is calculated using the 1-D Levenberg–Marquardt algorithm form [34] with the aim of minimizing the cost function. This algorithm was selected from among various algorithms for its fast convergence properties, as shown in Section III-B. For updated weights, the cost function is calculated in the forward pass; and, the whole procedure is carried out again until the desired performance is met or the NN starts failing the validation procedure, drifting away from the generalization criterion.

B. Selection of Predistorter Model Based on RVRNN and RVFTDNN Performances

The training procedure for the aforementioned networks is based on the realistic dynamic characterization of the PA fed with a modulated input signal. The device-under-test (DUT) was a highly nonlinear 54-dBm saturation power Doherty PA with a small-signal gain of 38 dB, driven with a third-generation (3G) signal (2.13–2.15-GHz band). 20 000 (20 K) data of a two-carrier WCDMA signal (PAPR = 10.5 dB, chip rate = 3.84 Mc/s) was used for training. For validation, 40 000 (40 K) data, which were purposely selected from different segments of the overall collected test data, were used.

Model identification and validation carried out in a MATLAB environment. The numbers of neurons in the two hidden layers, which were decided by the optimization process [16], were seven and 15 for the RVFTDNN and ten and 17 for the RVRNN. The output layer contains two linear neurons.

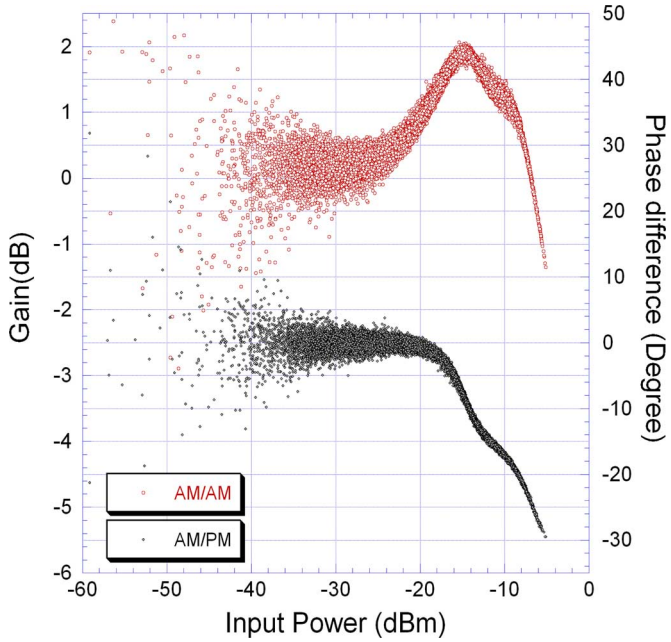

Fig. 4. AM/AM and AM/PM characteristics for Doherty PA.

TABLE I
COMPARISON OF RVRNN AND RVFTDNN MODELS

Model	Optimal No. of Neurons	No. of Delay Taps		Normalized Mean Square Error (dB)
		Input	Feedback	
RVRNN	10-17-2	3	1	-29
RVFTDNN	7-15-2	3	-	-38

Fig. 4 shows the AM/AM characteristics of the actual Doherty amplifier, depicting its highly nonlinear behavior. Scattering in the gain and phase characteristics due to multiple values of gain and phase for a single value of input power indicate the presence of memory effects in the PA. The RVFTDNN model was found to be the more accurate model with a normalized mean square error (NMSE) of -38 dB compared to -29 dB achieved with RVRNN, as shown in Table I.

On close inspection of Fig. 5(a), it is clear that the RVRNN is not capable of good modeling during the fast transition states of the waveform, while the RVFTDNN, as shown in Fig. 5(b), shows the capability for good modeling throughout the region. This difference is also visible in the time domain phase plot in Fig. 5(c) and (d). From Fig. 5(e), it can again be seen that the RVRNN has good modeling capability only for in-band data. These results corroborate those of the RNN reported in [24]. On the other hand, the RVFTDNN provides good accuracy in terms of power spectrum density for the full frequency range [see Fig. 5(f)].

The limited performance of the RVRNN can be understood from two facts. First, input to the RVRNN model is partially dependent on the model itself due to its recursive nature, which is evident from (1)–(3). This makes convergence slow during initial epochs when the NN is untrained. Second, the PA that we are trying to model here is part of an open loop transmitter system that does not have control feedback from output to input.

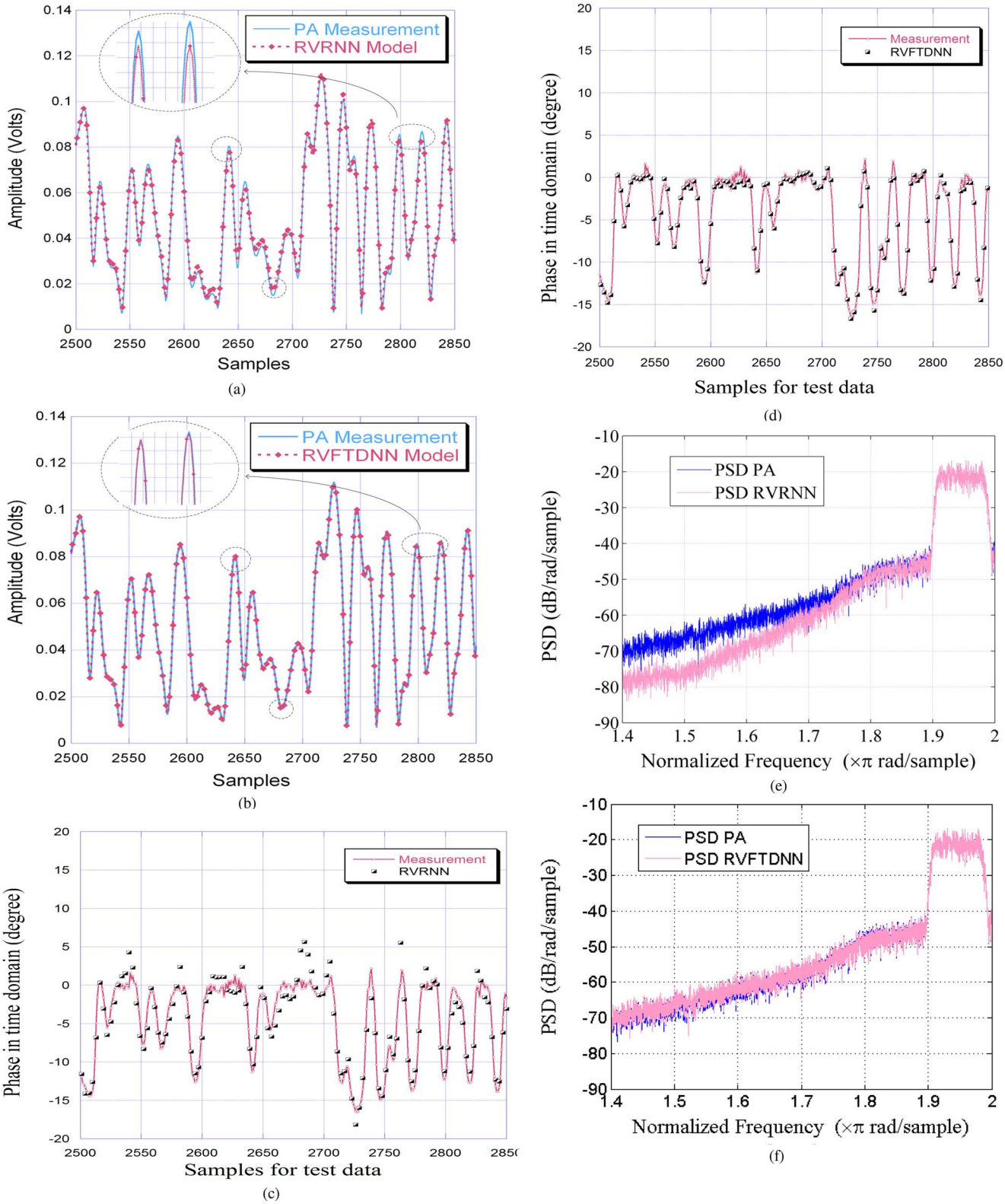

Fig. 5. Validation of: (a) RVRNN model, (b) RVFTDNN model for a WCDMA signal output voltage envelope in time domain, (c) RVRNN model for output phase in time domain, (d) RVFTDNN model for output phase in time domain, (e) power spectrum density plot of the RVRNN model output compared to the actual PA output, and (f) power spectrum density plot of the RVFTDNN model output compared to the actual PA output.

In this way, the RVFTDNN is closer to the physical analogy of the PA.

It is worth mentioning that the RVRNN and RVFTDNN are based on feedforward NNs; and, due to the universal approximation theorem, the RVRNN may eventually be able to give as good a performance as the RVFTDNN if we optimize it further and use a very high number of epochs. However, this will use more time and resources, taking away some of the advantage

TABLE II
PROMINENT BACK-PROPAGATION TECHNIQUES USED FOR NN TRAINING

Acronym	Algorithm
BFG	BFGS quasi-Newton
CGB	Powell-Beale conjugate gradient
CGF	Fletcher-Powell conjugate gradient
CGP	Polak-Ribiere conjugate gradient
GDA	Variable learning rate
GDM	Gradient descent with momentum
GDX	Momentum and adaptive learning rule
LM	Levenberg-Marquardt
OSS	On step secant
RP	Resilient back-propagation
SCG	Scaled conjugate gradient

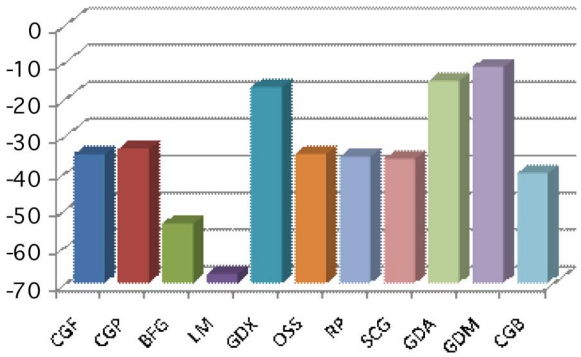

Fig. 6. Convergence of the NN model for different training algorithms after 50 epochs in terms of MSE (dB).

of using real-valued weights. Furthermore, the introduction of the feedback connection and delay loops adds additional complexity and uncertainty during initial epochs, leading to greater time and memory consumption, which is not effective for its performance, as indicated from the results. It can be concluded that the RVFTDNN offers a better, simple, and effective solution for the dynamic forward and reverse modeling of the PA.

C. Selection of the Training Algorithm

The extent of linearity improvement achieved by DPD depends mainly on the extraction of reverse characteristics of the PA, which implies that the error between the inverse characteristics and the output of the inverse model should be minimal. For a chosen topology, several training algorithms have been proposed in the NN literature [27]–[34], which enable the NN to achieve the required error minimization over some epochs. The adaptive predistortion puts a constraint on the number of epochs used for the whole learning process to achieve the optimal model, which, in turn, becomes a concern for the speed of convergence.

Faster back-propagation algorithms fall into two categories. The first category uses heuristic techniques, which were developed from an analysis of the performance of the standard steepest descent algorithm [16]. One heuristic modification is the momentum technique (GDM) [16], which eliminates the risk of falling into a shallow local minimum, while other modifications are variable learning rate back-propagation (GDA, GDX) and resilient back-propagation (RP).

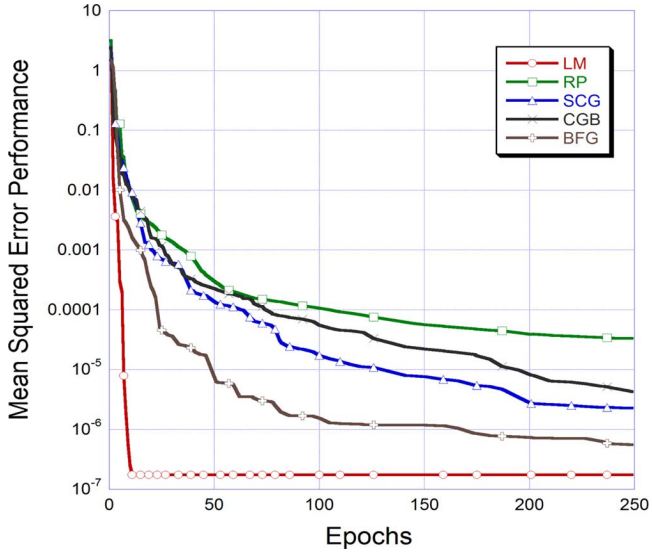

Fig. 7. Performance of the NN model for different training algorithms for 250 epochs in terms of MSE.

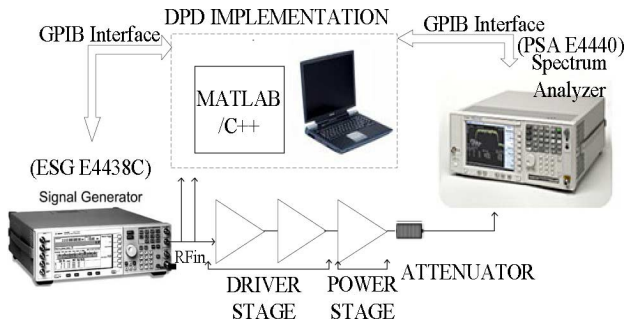

Fig. 8. Block diagram of measurement setup and predistorter implementation.

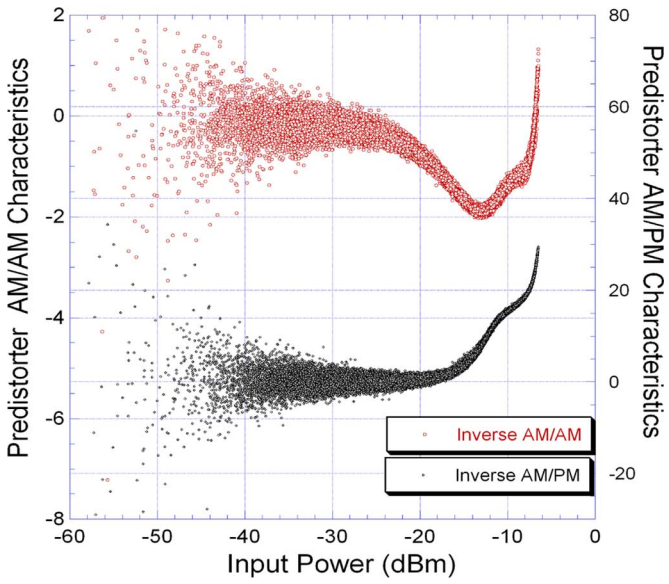

Fig. 9. Inverse modeling of a Doherty amplifier by RVFTDNN for the WCDMA11signal.

The second category of fast algorithms uses standard numerical optimization techniques [32] that cover three types of numerical optimization techniques for NN training, i.e., conjugate gradients (CGF, CGP, CGB, SCG) [29]–[33],

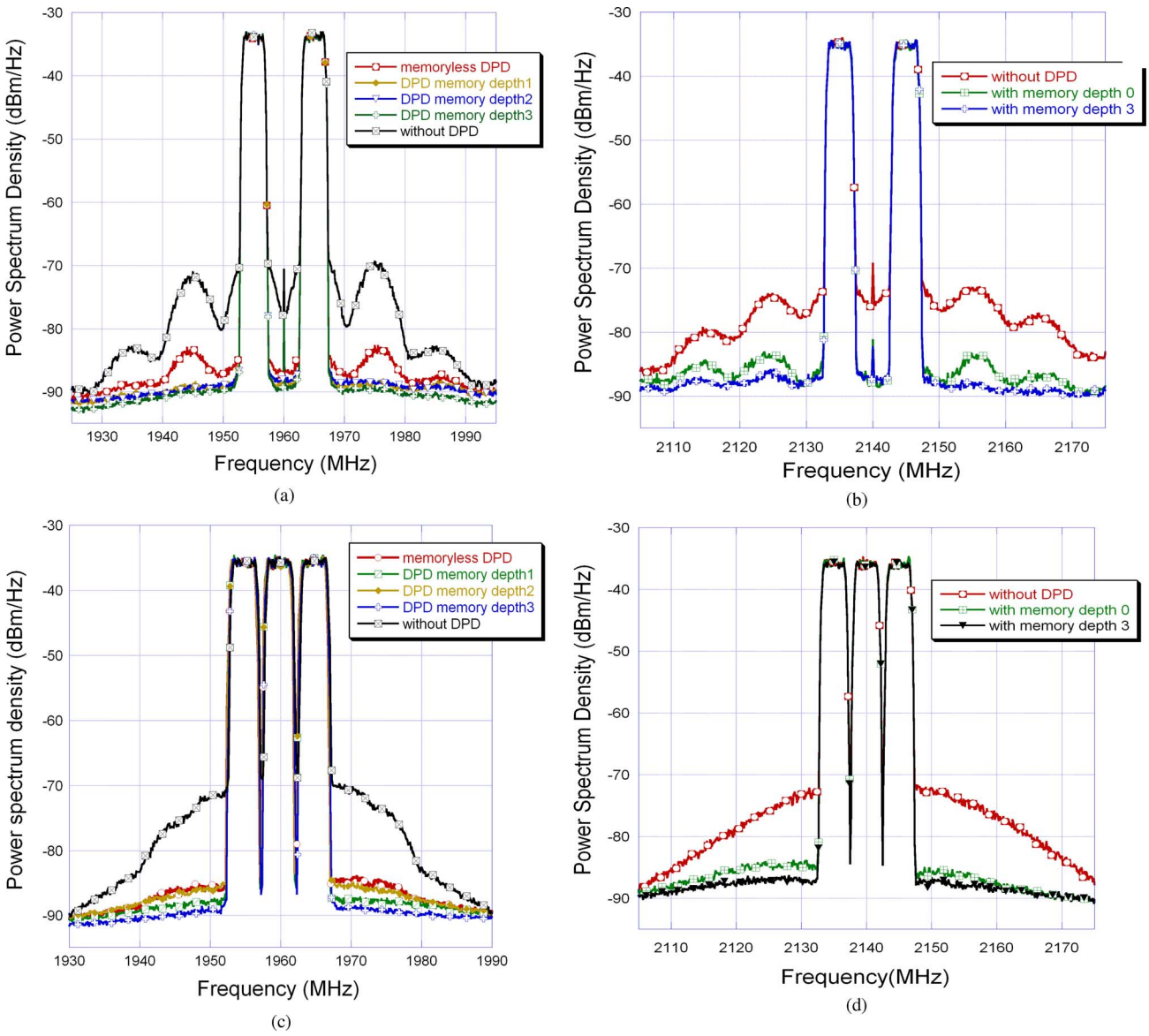

Fig. 10. Predistorter performance in terms of ACLR correction for: (a) a class AB amplifier with a WCDMA 101 signal, (b) a Doherty amplifier with a WCDMA 101 signal, (c) a class AB amplifier with a WCDMA 111 signal, and (d) a Doherty amplifier with a WCDMA 111 signal.

quasi-Newton (BFG, OSS) algorithms and the Levenberg–Marquardt algorithm (LM) [34]. Table II summarizes the prominent back-propagation techniques used for NN training.

These techniques were analyzed for fast and narrow error convergence. Data was extracted from a 54-dBm saturation power Doherty amplifier excited by a two-carrier WCDMA signal. All the algorithms were used for the NN according to RVFTDNN topology and were implemented in a MATLAB environment. Fig. 6 shows the mean square error (MSE) performance in decibels (dB) of the model utilizing various algorithms after 50 epochs. MSE was calculated as the average for ten trials with different initial conditions to convey a general trend of minimization capability.

As seen from the graph in Fig. 6, the numerical optimization techniques, like LM, BFG, and CGB, are narrowed down to much smaller values than the conventional gradient descent methods.

For fast operation as an adaptive predistorter, the NN should be able to converge in the least number of epochs. Fig. 7 shows that the convergence rate of other methods was significantly less than the LM algorithm, leading to high epoch counts and greater time consumption to extract the optimal model. The LM back-propagation algorithm was chosen as the most suitable algorithm since it achieved an MSE performance of 1.76×10^{-6} within 15 epochs.

IV. Experimental Measurement Setup and Implementation of DPD Based on RVFTDNN

For measurement and experimental validation purposes, the proposed RVFTDNN-based DPD model was implemented in a MATLAB/Advanced Design System (ADS) platform and used to linearize real PAs. Fig. 8 shows the experimental setup representing a linearized base station transmitter for 3G WCDMA signals.

TABLE III
ACLR ACHIEVED WITH THE LINEARIZATION OF PAs

3G Signals		CLASS AB POWER AMPLIFIER						DOHERTY POWER AMPLIFIER					
		± 5 MHZ OFFSET (dBc)		± 10 MHZ OFFSET (dBc)		± 15 MHZ OFFSET (dBc)		± 5 MHZ OFFSET (dBc)		± 10 MHZ OFFSET (dBc)		± 15 MHZ OFFSET (dBc)	
		LOW	HIGH	LOW	HIGH	LOW	HIGH	LOW	HIGH	LOW	HIGH	LOW	HIGH
WCDMA101	No DPD	45.05	45.39	36.99	35.31	49.16	48.57	40.65	41.42	39.09	37.91	45.67	43.52
	Static DPD	53.68	54.05	49.89	49.29	54.90	54.23	50.62	50.14	48.55	48.99	51.88	52.61
	Dynamic DPD	55.45	54.58	55.44	54.81	56.46	55.55	52.93	51.93	53.11	53.11	53.27	54.37
WCDMA111	No DPD	36.26	35.04	40.12	38.23	47.90	47.08	37.38	36.64	39.66	38.55	42.74	40.58
	Static DPD	50.01	49.71	50.59	49.25	53.30	51.83	49.69	49.56	48.89	49.35	49.60	50.97
	Dynamic DPD	53.10	53.15	54.59	53.88	54.93	53.33	51.64	51.76	51.92	52.52	51.89	52.67

The generated predistorted signals were downloaded in a signal generator (Agilent, ESG4438C) and then modulated and up-converted to RF and fed to the PA. The signal generator itself acted as a baseband modulator and RF up-converter with an ADS/MATLAB based digital signal processing (DSP) platform used for generating complex modulated signals. Together with a vector signal analyzer (Agilent, PSAE4440), the same setup shown in Fig. 8 could be used for characterizing the PA to retrieve its nonlinear characteristics. The output of the PA was down-converted to IF and sampled to obtain the I and Q components of the complex modulated signal from the output of the PA. The input and output complex waveforms were then used to find the time delay by correlating the waveforms and to time adjust in order to derive the nonlinear complex gain characteristics of the PA, which were used to obtain the DPD nonlinear complex gain characteristics with the MATLAB/ADS software platform.

In order to obtain the optimal back-off for the predistorter that would not change the peak and average power at which the PA characterization was performed, a power tracking scheme was implemented according to [35]. This ensured that the PA characteristics and the average power did not change significantly when the predistorter was introduced and that the peak-to-average power ratios (PAPRs) of the input and transmitted signals at the output of the linearized PA were approximately equal. A very small variation in average power could be tolerated, assuming the PA behavior herein was insensitive to power variation of less than 0.5 dB [26], [35].

The RVFTDNN was trained to extract the normalized inverse characteristics according to

$$X_{\text{in}} = f^{-1}(y_{\text{norm}}) \tag{10}$$

where y_{norm} denotes the vector containing the I and Q components for the PA output at that instance and previous instances (the memory length was decided by an optimization process) after normalizing it with a small-signal complex gain (achieved during the characterization process of the PA), and X_{in} denotes the vector containing the I and Q components of the input to the PA at that instance.

Fig. 9 shows the inverse characteristics of a Doherty PA (PA characteristics shown in Fig. 4) obtained by the RVFTDNN. A fixed interval predistorter was updated with new weights and adjuster settings to make it more robust for the PA characteristics

TABLE IV
MSE PERFORMANCE OF REVERSE MODEL WITH DIFFERENT SIGNALS

3G Signal	Trained for WCDMA1 MSE(dB)	Trained for WCDMA11 MSE(dB)	Trained for WCDMA111 MSE(dB)
WCDMA1	-57.92	-58.29	-58.98
WCDMA11	-57.20	-57.80	-57.93
WCDMA101	-55.07	-56.20	-56.46
WCDMA111	-55.94	-55.93	-57.47
WCDMA1001	-51.12	-55.22	-56.16
WCDMA1111	-51.70	-53.34	-54.16

that slowly change due to environmental condition and temperature variations. The weight updating interval depends on the feedback loop training duration in the software being used to synthesize the predistorter. In light of this fact, the predistorter weights need to be updated every 5 min while processing in MATLAB and can be reduced to less than 1 min when efficiently implemented in a dedicated processor.

The proposed predistorter was implemented in MATLAB, and predistorted signals were used to linearize a mildly nonlinear 1.96-GHz class AB amplifier and a strongly nonlinear 2.14-GHz Doherty amplifier with memory effects. The class AB PA had a saturation power of 40 dBm with a gain of approximately 42 dB. The Doherty amplifier had a saturated power of 54 dBm and a small-signal gain of approximately 38 dB. Both of the PAs were linearized for multicarrier WCDMA signals with a PAPR of 10.5 dB.

V. MEASUREMENT RESULTS AND DISCUSSION

The proposed predistortion scheme was first implemented with a 1.96-GHz class AB amplifier, which, in turn, was excited with WCDMA101 (three-carrier WCDMA signal with the center carrier off) and WCDMA111 (WCDMA signal with all three carriers present) signals.

Fig. 10 shows power spectrum density curves for the Doherty and class AB amplifiers with various signals. Each graph shows the linearized PA output spectrum with and without DPD correction. The curves also indicate the effect of memory consideration in the proposed model in terms of ACLR reduction. A static DPD indicates the RVFTDNN structure with no tapped line. It

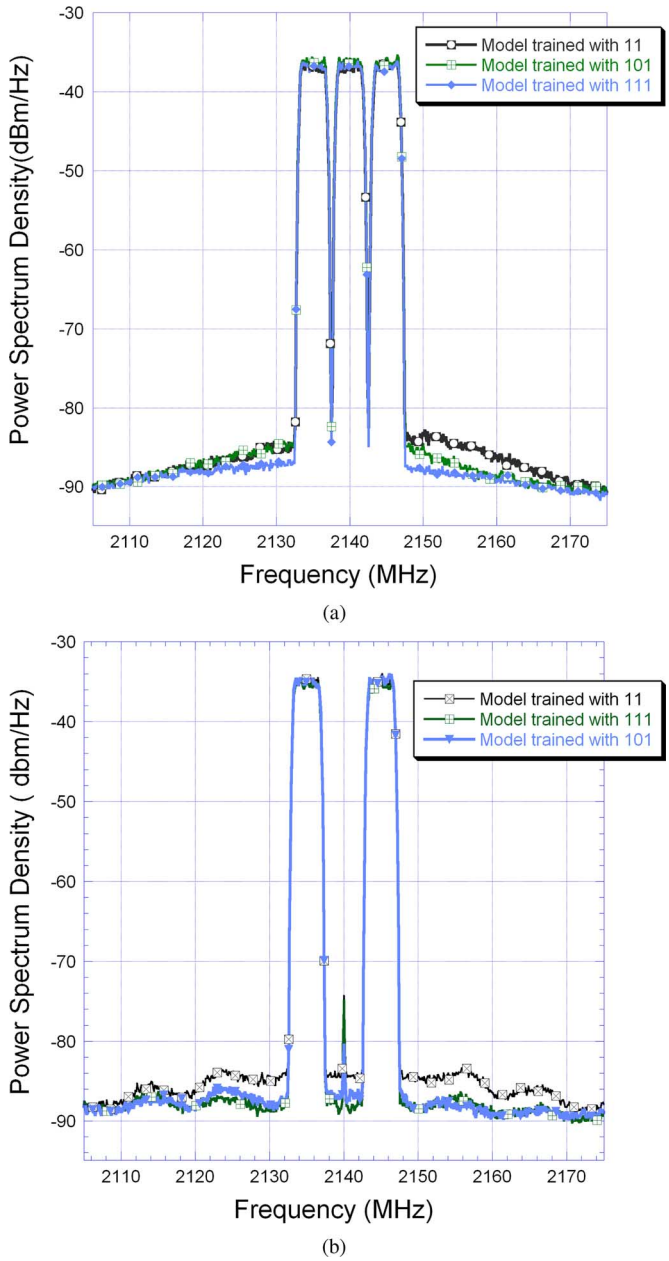

Fig. 11. Predistorter performance in terms of ACLR correction for: (a) effect of training signal on linearization tested with a WCDMA111 signal and (b) effect of training signal on linearization tested with a WCDMA101 signal.

is clear from Fig. 10 that the performance of the predistorter was significantly affected by its dynamic modeling capabilities. The best performance was achieved for the delay line with memory depth 3. Table III summarizes the ACLP achieved for different amplifiers and signals at 5-, 10-, and 15-MHz frequency offset. The robustness of the model was also validated by applying different signals that were not used in the training procedure for the models.

Table IV gives the MSE performance of the inverse model (trained with different signals) output for the different signals and the actual output signal for which it was trained. From this table, the models were observed to be backward compatible in the sense that the model trained with a WCDMA1 signal was not optimal when used with other signals, while the model trained for a WCDMA111 signal kept its performance for signals with fewer carriers. In light of this new fact, the predistorter weight updating interval was modified to update the weights before the predefined fixed interval if signal was switched with a high-carrier signal. The practical measurement results also corroborated this fact, as shown in Fig. 11.

As mentioned in Section IV, all WCDMA signals had PAPRs of about 10.5 dB, and the output power of the linearized PA was approximately the same for all signals used. The linearization was achieved for an output power back-off (OPBO) relative to the saturation point which is equal to the PAPR of the signal plus the gain expansion of the predistorter (which shall be equal to the gain compression of the PA). In such conditions, clipping and overdriving the linearized PA are avoided. For the Doherty PA, the linearized PA was operated at 13.5-dB OPBO, equal to the sum of 10.5-dB PAPR of the signal and about 3 dB of a gain compression. The quasi-perfect nonlinearity cancellation was achieved, requiring the increase of the OPBO by 3 dB. In contrast, based on Fig. 4, operating the PA in far back-off (30 dB or deeper for the average power) to ensure linear operation for the whole dynamic range of the signal led to a comparable linearity performance, but with a significant measured power efficiency reduction to less than 5% as compared to 20% for the linearized PA.

VI. Conclusion

This paper presents an adaptive predistortion technique based on an RVFTDNN for the linearization of 3G baseband PA. The appropriate neural network topology was selected by comparing the RVFTDNN and an RVRNN. A comparative study of various training algorithms was carried out to select the most appropriate algorithm to incorporate fast and accurate convergence. Finally, for the first time, to the best knowledge of the authors, a predistortion scheme based on the RVFTDNN was validated using a real test-bed environment. The linearization capability of the RVFTDNN predistorter with a real PA was validated for a class AB PA, as well as for a highly nonlinear Doherty amplifier, where the amplifier was excited with both single-carrier and multicarrier WCDMA signals. The measurement results confirm the influence of memory effect on the overall predistorter performance in the context of a real-valued NN.

Acknowledgment

The authors would like to acknowledge the team at the iRadio Laboratory, University of Calgary, Calgary, AB, Canada, and its sponsors for their support.

References

[1] P. B. Kenington, *High-Linearity RF Amplifier Design*. Boston, MA: Artech House, 2000.
[2] E. E. Eid, F. M. Ghannouchi, and F. Beauregard, "Optimal feedforward linearization system design," *Microw. J.*, vol. 38, no. 11, pp. 78–86, 1995.
[3] Y. W. Young, Y. Youngoo, Y. Jaehyok, N. Joongjin, H. C. Jeong, and K. Bumman, "Feedforward amplifier for WCDMA base stations with a new adaptive control method," in *IEEE MTT-S Int. Microw. Symp. Dig.*, Seattle, WA, Jun. 2002, vol. 2, pp. 769–772.
[4] Y. Kim, Y. Yang, S. H. Kang, and B. Kim, "Linearization of 1.85 GHz amplifier using feedback predistortion loop," in *IEEE MTT-S Int. Microw. Symp. Dig.*, Baltimore, MD, 1998, pp. 1675–1678.

[5] A. K. Ezzeddine, H. A. Hung, and H. C. Huang, "An MMAC C-band FET feedback power amplifier," *IEEE Trans. Microw. Theory Tech.*, vol. 38, no. 4, pp. 350–357, Apr. 1990.
[6] K. A. Morris and J. P. McGeehan, "Gain and phase matching requirements of cubic predistortion systems," *Electron. Lett.*, vol. 36, no. 21, pp. 1822–1824, Oct. 2000.
[7] W. Woo, M. D. Miller, and J. S. Kenney, "A hybrid digital/RF envelope predistortion linearization system for power amplifiers," *IEEE Trans. Microw. Theory Tech.*, vol. 53, no. 1, pp. 229–237, Jan. 2005.
[8] P. B. Kennington, "Linearized transmitters: An enabling technology for software defined radio," *IEEE Commun. Mag.*, vol. 40, pp. 156–162, Feb. 2002.
[9] K. J. Muhonen, M. Kavehrad, and R. Krishnamurthy, "Look-up table techniques for adaptive digital predistortion: A development and comparison.," *IEEE Trans. Veh. Technol.*, vol. 49, no. 9, pp. 1995–2002, Sep. 2000.
[10] J. K. Cavers, "Amplifier linearization using a digital predistorter with fast adaptation and low memory requirements," *IEEE Trans. Veh. Technol.*, vol. 39, no. 4, pp. 374–382, Nov. 1990.
[11] A. Zhu and J. C. Pedro, "Amplifier distortion evaluation of RF power amplifiers using dynamic deviation reduction based volterra series," in *IEEE MTT-S Int. Microw. Symp. Dig.*, 2007, pp. 965–968.
[12] H. W. Kang, Y. S. Cho, and D. H. Youn, "Adaptive precompensation of wiener systems," *IEEE Trans. Signal Process.*, vol. 46, no. 10, pp. 2825–2829, Oct. 1998.
[13] M. Ghaderi, S. Kumar, and D. E. Dodds, "Fast adaptive predistortion linearizer using polynomial functions," *Electron. Lett.*, vol. 29, no. 17, pp. 1526–1528, 1993.
[14] D. R. Morgan, M. Zhenngxiang, L. Kim, M. G. Zierdt, and I. Pastalan, "A generalized memory polynomial model for digital predistortion of RF power amplifiers," *IEEE Trans. Signal Process.*, vol. 54, no. 10, pp. 3852–3860, Oct. 2006.
[15] Q. J. Zhang and K. C. Gupta, *Neural Networks for RF and Microwave Design*. Norwood, MA: Artech House, 2000.
[16] S. Haykin, *Neural Networks: A Comprehensive Foundation*. Upper Saddle River, NJ: Prentice-Hall, 1999.
[17] Y. Bengio, *Neural Networks for Speech and Sequence Recognition*. New York: ITC Press, 1995.
[18] K. S. Narendra and K. Parthasarathy, "Identification and control of dynamical systems using neural networks," *IEEE Trans. Neural Netw.*, vol. 1, no. 1, pp. 4–27, Mar. 1990.
[19] J. J. Xu, M. C. E. Yagoub, R. T. Ding, and Q. J. Zhang, "Neural-based dynamic modeling of nonlinear microwave circuits," *IEEE Trans. Microw. Theory Tech.*, vol. 50, no. 12, pp. 2769–2780, Dec. 2002.
[20] M. Ibnkahla, J. Sombrin, F. Castanie, and N. J. Bershad, "Neural networks for modeling nonlinear memoryless communication channels," *IEEE Trans. Commun.*, vol. 45, no. 7, pp. 768–771, Jul. 1997.
[21] N. Benvenuto, F. Piazza, and A. Uncini, "A neural network approach to data predistortion with memory in digital radio systems," in *Proc. IEEE Int. Commun. Conf.*, Singapore, Nov. 1995, vol. 1, pp. 152–156.
[22] N. Naskas and Y. Papananos, "Adaptive baseband predistorter for radio frequency power amplifiers based on a multilayer perceptron," in *9th Int. Electron.. Circuits, Syst. Conf.*, 2002, vol. 3, no. 11, pp. 1107–1110.
[23] Y. Quian and F. Liu, "Neural network predistortion technique for nonlinear power amplifiers with memory," in *1st Int. Commun. Networking in China Conf.*, Oct. 2006, pp. 1–5.
[24] D. Luongyinh and Y. Kwon, "Behavioral modeling of power amplifiers using fully recurrent neural networks," *IEEE MTT-S Int. Microw. Symp. Dig.*, pp. 1979–1982, Jun. 2005.
[25] T. Liu, S. Boumaiza, and F. Ghannouchi, "Dynamic behavioral modeling of 3G power amplifiers using real-valued time-delay neural networks," *IEEE Trans. Microw. Theory Tech.*, vol. 52, no. 3, pp. 1025–1033, Mar. 2004.
[26] J. Vuolevi, T. Rahkonen, and J. Manninen, "Measurement technique for characterizing memory effects in RF power amplifiers," *IEEE Trans. Microw. Theory Tech.*, vol. 49, no. 8, pp. 1383–1389, Aug. 2001.
[27] R. Hecht-Nielsen, "Theory of the back propagation neural network," in *Proc. Int. Joint Neural Netw. Conf.*, Jun. 1989, Art. ID I-593-60.
[28] R. Battiti, "First and second order methods for learning: Between steepest descent and Newton's method," *Neural Comput.*, vol. 4, no. 2, pp. 141–166, 1992.
[29] E. M. L. Beale, "A derivation of conjugate gradients," in *Numerical Methods for Nonlinear Optimization*, F. A. Lootsma, Ed. London, U.K.: Academic, 1972.
[30] J. E. Dennis and R. B. Schnabel, *Numerical Methods for Unconstrained Optimization and Nonlinear Equations*. Englewood Cliffs, NJ: Prentice-Hall, 1983.
[31] R. Fletcher and C. M. Reeves, "Function minimization by conjugate gradients," *Comput. J.*, vol. 7, pp. 149–154, 1964.
[32] M. T. Hagan, H. B. Demuth, and M. H. Beale, *Neural Network Design*. Boston, MA: PWS Publishing, 1996.
[33] M. F. Moller, "A scaled conjugate gradient algorithm for fast supervised learning," *Neural Netw.*, vol. 6, pp. 525–533, 1993.
[34] M. T. Hagan and M. B. Menhai, "Training feedforward network with the Marquardt algorithm," *IEEE Trans. Neural Net.*, vol. 5, no. 6, pp. 989–993, Nov. 1994.
[35] O. Hammi, S. Boumaiza, and F. M. Ghannouchi, "On the robustness of digital predistortion function synthesis and average power tracking for highly nonlinear power amplifier," *IEEE Trans. Microw. Theory Tech.*, vol. 55, no. 6, pp. 1382–1389, Jun. 2007.

Meenakshi Rawat (S'09) received the B.Tech. degree in electrical engineering from Govind Ballabh Pant University of Agriculture and Technology, Pantnagar, Uttaranchal, India, in 2006, and is currently working toward the M.Sc. degree in electrical and computer engineering at the Schulich School of Engineering, University of Calgary, Calgary, AB, Canada.

She was associated with the Telco Construction Equipment Company Ltd., Jamshedpur, India (2006–2007) and Hindustan Petroleum Corporation Limited (HPCL), Noida, India (2007–2008). She is now with the iRadio Laboratory, Schulich School of Engineering, University of Calgary, as a Student Research Assistant. Her current research interest is in the area of microwave active and passive circuit modeling using NNs.

Karun Rawat (S'09) received the B.E. degree in electronics and communication engineering from Meerut University, Uttar Pradesh, India, in 2002, and is currently working toward the Ph.D. degree in electrical and computer engineering at the Schulich School of Engineering, University of Calgary, Calgary, AB, Canada.

From 2003 to 2007, he was with the Indian Space Research Organization. He then joined the iRadio Laboratory, Schulich School of Engineering, University of Calgary, where he is a Student Research Assistant. His current research interests are in the areas of microwave active and passive circuit design and advanced transmitter and receiver architecture for software-defined radio applications.

Fadhel M. Ghannouchi (S'84–M'88–SM'93–F'07) is currently a Professor and iCORE/CRC Chair with the Department of Electrical and Computer Engineering, Schulich School of Engineering, University of Calgary, Calgary, AB, Canada, and Director of the Intelligent RF Radio (iRadio) Laboratory. He has held numerous invited positions with several academic and Research institutions in Europe, North America, and Japan. He has provided consulting services to a number of microwave and wireless communications companies. His has authored or coauthored over 400 publications. He holds ten U.S. patents with three pending. His research interests are in the areas of microwave instrumentation and measurements, nonlinear modeling of microwave devices and communications systems, design of power and spectrum efficient microwave amplification systems, and design of intelligent RF transceivers and SDR radio systems for wireless and satellite communications.